Measurement of Interprotein Distances in the Acto–Subfragment 1 Rigor Complex†

Reiji Takashi* and Andrzej A. Kasprzak*
Cardiovascular Research Institute, University of California, San Francisco, San Francisco, California 94143
Received April 15, 1987; Revised Manuscript Received July 7, 1987

ABSTRACT: Using enzymatic labeling, we have conjugated the fluorescence probe dansylcadaverine (DNC) to Gln-41 of rabbit skeletal muscle actin with the intention of utilizing the dansyl chromophore as a donor in fluorescence resonance energy transfer (FRET) distance measurements. The fluorescence decay of DNC–actin was found to consist of two decay constants (8.23 and 21.2 ns) that were associated with two different but partially overlapping spectra of the dye. Three different chemical points on myosin subfragment 1 (S1) were labeled with suitable acceptors: reactive thiol 1 (SH_1) and Cys-136 on LC_3 were modified with tetramethylrhodamine 5- (and 6-) iodoacetamide (ITMR); Lys-83 (RLR) was derivatized with trinitrobenzenesulfonate. In the rigor complex of the two labeled proteins, fluorescence resonance energy transfer took place, the efficiency of which was 10.9, 9.28, and 3.73% for the transfer from Gln-41 to SH_1, Cys-136 (LC_3), and RLR, respectively. The limits of the Förster critical distance for each pair were obtained from the analysis of the polarization spectra of the donor and of the acceptors. The $\kappa^2(2/3)$ distances from actin Gln-41 to the three points on S1 were 63, 66, and >37 Å for SH_1, Cys-136 (LC_3), and RLR, respectively.

The elucidation of the molecular architecture of the myosin–actin complexes is the first step toward understanding the mechanism through which muscle contraction occurs. Because a high-resolution X-ray structure of the actomyosin or acto–S1[1] complexes is not available and there is little hope that it will be available in the near future, for over a decade various laboratories have used fluorescence energy transfer and electron microscopy to obtain information about the geometry of the complex and proximity of chemically defined points on both proteins (Moore et al., 1970; Taylor & Amos, 1981; Sutoh et al., 1984, 1986; Toyoshima & Wakabayashi, 1985; Winkelman & Lowey, 1986; Miki & Mihashi, 1978; Takashi, 1979; Marsh & Lowey, 1980; Tao & Lamkin, 1981; Takashi et al., 1982, 1984; Moss & Trentham, 1983; Dalbey et al., 1983; Cheung et al., 1983; Miki & Wahl, 1984; Dos Remedios & Cooke, 1984). A three-dimensional map of the acto–S1 complex has subsequently been assembled in our laboratory (Botts et al., 1984) and employed a number of times to design experiments in order to test various hypotheses concerning the mechanism of transduction. Examination of the map shows, however, that there are only two points on actin whose distances to points on S1 have been determined, viz., the actin nucleotide binding site and Cys-374. The scarcity of points is mainly due to the fact that a limited number of residues on actin can be specifically modified with at least partial preservation of the protein's biological function, such as polymerization, binding of nucleotides, etc.

Recently, a new method of enzymatic conjugation of fluorescence probes to Gln-41 of actin has been developed (Takashi, 1987). The modification appears to be almost completely innocuous to the protein leaving all its biological properties virtually unaffected.

The availability of this labeled actin enabled us to perform fluorescence energy transfer experiments designed to determine the distances from Gln-41 on actin to three well-known loci on S1 in the actomyosin complex: reactive thiol 1 (SH_1), Lys-83 (reactive lysine residue, RLR) (Tong & Elzinga, 1983), and Cys-136 on light chain 3 (Franks & Weeds, 1974). Preliminary values of these distances have been reported before (Takashi & Kasprzak, 1985).

Materials and Methods

Chemicals. Tetramethylrhodamine 5- (and 6-) iodoacetamide (ITMR) was purchased from Molecular Probes (Eugene, OR). 2,4,6-Trinitrobenzenesulfonic acid (TNBS) and dansylcadaverine were obtained from Sigma. Ion-exchange celluloses (DE-52 and SE-53) were from Whatman. Ultrapure guanidine hydrochloride was from Schwarz/Mann. All other reagents were of analytical grade.

Proteins. Rabbit skeletal muscle actin was prepared as described by Spudich and Watt (1971). Subfragment 1 (S1) from rabbit skeletal muscle was isolated following the procedure of Weeds and Taylor (1975). Isozymes of S1 [S1(LC_1) and S1(LC_3)] were separated on an SE-53 column (Trayer & Trayer, 1983) and dialyzed against 10 mM TES containing 0.1 M NaCl, pH 7.0, overnight. Guinea pig liver transglutaminase was prepared as described by Connellan et al. (1971). A mixture of all three light chains was prepared from rabbit skeletal myosin according to the method of Holt and Lowey (1975). The alkali light chains were further separated on a (carboxymethyl)cellulose HPLC column ([TSK-535CM, LKB (Bromma, Sweden)].

Labeling SH_1 of S1 with Tetramethylrhodamine 5- (and 6-) Iodoacetamide. S1 (50 μM) was incubated with a 6-fold molar excess of ITMR in a solution containing 20 mM TES, 0.1 M NaCl, and 5 mM $MgCl_2$, pH 7.0, on ice in the dark for 2 h. A large excess of β-mercaptoethanol was then added,

† This work was supported by a grant from the National Science Foundation (NSF PCM 8316007) and by National Institutes of Health Program Project Grant HL-16683.

[1] Abbreviations: DTT, dithiothreitol; IAA, iodoacetamide; ITMR, tetramethylrhodamine 5- (and 6-) iodoacetamide; TNP, trinitrophenol; TNBS, trinitrobenzenesulfonate; SH_1, reactive thiol 1; RLR, reactive lysine residue, Lys-83 of S1; LC_3, alkali light chain 3; LC_1, alkali light chain 1; DNC, dansylcadaverine; TMR, tetramethylrhodamine 5- (and 6-) acetamido derivative; 1,5-IAEDANS, *N*-(iodoacetyl)-*N'*-(5-sulfo-1-naphthyl)ethylenediamine; S1, myosin subfragment 1; Gdn-HCl, guanidine hydrochloride; FRET, fluorescence resonance energy transfer; TES, 2-[[tris(hydroxymethyl)methyl]amino]ethanesulfonic acid; HPLC, high-performance liquid chromatography; Tris-HCl, tris(hydroxymethyl)aminomethane hydrochloride.

0006-2960/87/0426-7471$01.50/0

and the protein was separated on a Sephadex G-25 column that had been equilibrated with 10 mM TES, 50 mM KCl, 1 mM $MgCl_2$, and 0.5 mM DTT, pH 7.5. After an overnight dialysis, labeled S1 was centrifuged at 130000*g* for 30 min.

Labeling of LC_3 with Tetramethylrhodamine 5- (and 6-) Iodoacetamide. The single cysteine residue of light chain 3 (Cys-136) was labeled with ITMR essentially as in Marsh and Lowey (1980). TMR-labeled LC_3 was then exchanged into $S1(LC_1)$ by the method of Wagner and Weeds (1976); TMR-labeled $S1(LC_3)$ was separated on a DE-52 column according to Weeds and Taylor (1975).

Labeling of RLR with TNBS was done as in Muhlrad and Takashi (1981). S1 labeled with iodoacetamide was prepared as described previously (Takashi et al., 1976).

Enzymatic modification of actin with dansylcadaverine will be described elsewhere (Takashi, 1987). Briefly, G-actin (50 μM) was incubated with dansylcadaverine (0.25 mM) and guinea pig liver transglutaminase (1 μM) for 20 h in 5 mM Tris-HCl buffer, pH 8.0, containing 1 mM DTT, 0.4 mM ATP, 1 mM $CaCl_2$, and 1 mM NaN_3 at 4 °C. The labeled actin was polymerized by the addition of 1 mM $MgCl_2$ and 50 mM KCl at 25 °C, and the F-actin was collected by centrifugation at 130000*g* for 60 min.

Labeling Stoichiometry. Stoichiometry of the dansylcadaverine binding to actin has been determined from the absorption of dansyl by assuming $\epsilon_{326nm} = 4.64 \times 10^3$ M^{-1} cm^{-1} (Lorand et al., 1968). The stoichiometry of S1 labeling with TNP has been determined from the absorbance at 345 nm by assuming an extinction coefficient of 1.45×10^4 M^{-1} cm^{-1} (Okuyama & Satake, 1960). The extinction coefficient of the TMR-S1 was determined as follows: A sample of ITMR was weighed out and reacted with *N*-acetyl-L-cysteine, and the extinction coefficient of the resulting conjugate was measured in 6 M Gdn-HCl. The effect of Gdn-HCl on the absorption spectrum of S1-bound TMR was determined, yielding a correction factor that has been applied to the extinction coefficient of the conjugate in Gdn-HCl. The final ϵ_{555nm} for TMR in buffer solution was found to be 5.0×10^4 M^{-1} cm^{-1}. For all labels the absorption values were corrected for the turbidity of the samples.

Protein Concentrations. The concentration of S1 was determined with $A_{280}^{1\%} = 7.5$ (Wagner & Weeds, 1977); for G-actin, $A_{290}^{1\%} = 6.30$ or $A_{280}^{1\%} = 11.1$ (Houk & Ue, 1974) was used. Concentrations of G-actin and S1 labeled with fluorescent probes were measured by the method of Lowry et al. (1951) with unlabeled S1 or G-actin as standards. Alternatively, the protein concentrations were determined from the absorbance at 280 nm. In the latter method, it was necessary to correct the protein absorption for the absorption of the label. The amount of correction was estimated by measuring the absorption of the probe at its absorption maximum and from this value calculating the contribution of the label to the total absorption at 280 nm. Molecular weights of S1 and G-actin were assumed to be 110000 (Margossian & Lowey, 1981) and 42000 (Elzinga et al., 1973).

Steady-state fluorescence spectra were obtained on an SLM 8000 fluorometer (SLM, Inc., Urbana, IL) operated in the ratio mode. The spectra were transferred on-line to an IBM XT microcomputer, where they were subsequently corrected for background and also for the wavelength dependence of the photomultiplier and emission monochromator with the SLM-supplied correction factors. To eliminate polarization bias in the recorded emission spectra, a polarizer oriented at 55° with respect to the vertical direction was placed in the excitation beam; the emission was recorded through a vertically oriented polarizer (Spencer & Weber, 1970). The buffer used for FRET measurements contained 10 mM TES, 50 mM KCl, 1 mM $MgCl_2$, and 0.5 mM DTT, pH 7.5.

For quantum yield measurements quinine sulfate in 0.1 N H_2SO_4 was used as a reference standard of $Q = 0.70$ (Scott et al., 1970).

Polarization spectra were recorded on the same instrument operated in T format and employing a set of Glan–Thomson prisms.

Fluorescence lifetimes were determined on a pulsed, single photon counting instrument whose optical components were purchased from PRA, Inc. (London, Ontario, Canada), and the data collection system was as described by Mendelson et al. (1975). Deconvolution of the technical fluorescence decay curves was accomplished by use of the nonlinear least-squares analysis package (Badea & Brand, 1975; Grinvald & Steinberg, 1974). Decay-associated spectra (DAS) were obtained as described earlier (Torgerson, 1984). The samples were excited through a combination of Schott UG1 and UG11 band-pass filters. To isolate emission wavelengths in the range 450–656 nm, Melles–Griot interference filters were employed.

The efficiency of the energy transfer E between probes was calculated from fluorescence lifetimes:

$$E = 1 - \tau_{DA}/\tau_D \quad (1)$$

where τ_{DA} and τ_D are the lifetimes of the donor in the presence and absence of the acceptor, respectively. This method was preferred over steady-state measurements since the fluorescence decay of actin-bound dansylcadaverine consists of more than one component and a number of experiments indicate that some molecules of dansylcadaverine are quenched by a static mechanism (A. A. Kasprzak and R. Takashi, unpublished results).

The critical Förster distance R_0 was calculated from

$$R_0^6 = (8.79 \times 10^{-5})\kappa^2 n^{-4} Q_D J \quad (2)$$

where Q_D is the quantum yield of the donor, J is the overlap integral, n is the refractive index of the medium in which the transfer takes place (assumed here to be equal 1.4), and κ^2 is the orientation factor. For dynamically isotropic motion of the probe during the fluorescence lifetime, $\kappa^2 = 2/3$.

Absorption spectra of the acceptors were obtained on a Cary 118C spectrophotometer interfaced to an IBM XT computer. The overlap integral J was obtained from the computer-accumulated fluorescence and absorption spectra by integration in 1-nm intervals with

$$J = \sum_\lambda F_D(\lambda)\epsilon_A(\lambda)\lambda^4 \, \Delta\lambda / \sum_\lambda F_D(\lambda) \, \Delta\lambda \quad (3)$$

where F_D denotes the corrected fluorescence intensity of the donor and ϵ_A is the molar absorption coefficient of the acceptor at wavelength λ. The distance between the donor and the acceptor, r_i, was calculated from

$$r_i = R_0[(1 - E)/E]^{1/6} \quad (4)$$

Results and Discussion

Specificity of the Labeling. Table I summarizes the properties of four preparations used for the present experiments. The labeling specificity of the reactive lysine residue with TNBS and isolated alkali light chains with iodoacetamide-based probes is well documented (Muhlrad & Takashi, 1981; Marsh & Lowey, 1980), and as expected, conjugation of the probes to these residues resulted in almost stoichiometric modification (Table I). For labeling of Gln-41 with transglutaminase, the number of moles of dansylcadaverine per mole of the enzyme approached a ratio of 1 with the specificity

Table I: Labeling Stoichiometry of Actin and S1 with Fluorescent Probes

		protein	probe	stoichiometry (mol/mol)
I	donor	actin	DNC	0.758
	acceptor	LC_3[a]	TMR	0.993
II	donor	actin	DNC	0.944
	acceptor	S1	TNP	0.957
III	donor	actin	DNC	0.976
	acceptor	S1	TMR	0.779
IV	donor	actin	DNC	0.610
	acceptor	S1	TMR	1.25

[a] LC_3 bound to S1 heavy chain.

of approximately 80–85% (Takashi, 1987). We note that stoichiometric labeling of actin is not crucial since molecules without dansyl are not seen in fluorescence experiments.

We have employed peptide mapping to determine the specificity of S1 labeling with ITMR. The dye has been localized only in the 20-kDa fragment of the protein. After tryptic digestion of S1, a single major peptide carrying TMR has been detected and purified on a reverse-phase HPLC column. The peptide had the sequence Ile-X-Arg, where X denotes the modified amino acid. Comparing this to the published sequence of the 20-kDa fragment of S1 (Elzinga & Collins, 1977; Gallagher & Elzinga, 1980) strongly suggests that X = Cys and the ITMR labeling is SH_1-specific.

Spectroscopic Properties of the Donor. Preparations of DNC–G-actin and DNC–F-actin show double-exponential fluorescence decays and have wavelength-dependent preexponential factors; Figure 1 shows an example of such a decay for F-actin. By determining the contributions of both components as a function of the emission wavelength, we were able to reconstruct the spectra associated with each of the two components of the decay (DAS). Figure 2 shows these spectra for F-actin and G-actin.

The question, of course, arises: What is the origin of these fluorescence components? Two components in the decay could originate from (a) two different labeling sites on actin, (b) incomplete solvent relaxation of the solvent molecules around the chromophore, or (c) heterogeneous interactions of the dye with the protein. This case includes interactions that are heterogeneous because actin consists of a mixed population of protein molecules that differ slightly in their conformation and interactions resulting from penetration of different environments by the dansyl chromophore.

Hypothesis a is in disagreement with the analysis of the specificity of the labeling performed by the peptide mapping (Takashi, 1987). As mentioned above, the specificity exceeds 85%, and nonspecific labeling cannot explain the present results. We have also prepared a sample that has been "lightly" labeled (n = 0.26 mol/mol). For this sample the labeling of only Gln-41 could be detected (results not shown). As evident from Table II, this sample also displayed a two-component decay curve. The ratio of the two components was similar to that for the fully labeled sample.

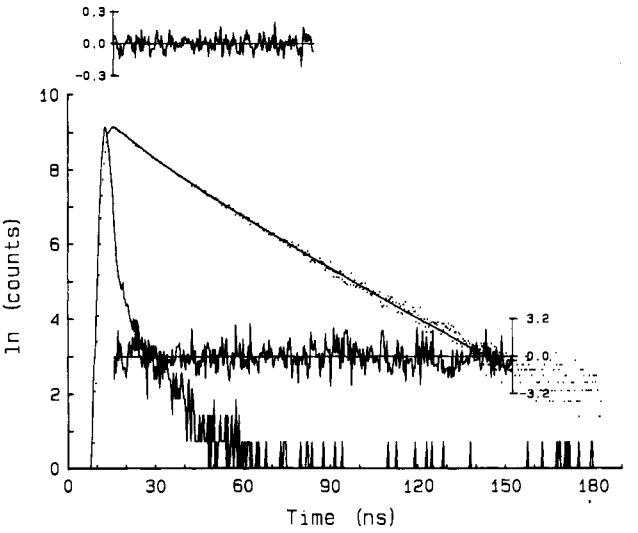

FIGURE 1: Nanosecond decay kinetics of dansylcadaverine–actin (12 μM) in 2 mM Tris, 1 mM $MgCl_2$, 0.2 mM $CaCl_2$, 0.2 mM ATP, 0.4 mM β-mercaptoethanol, and 0.1 M NaCl, pH 8.0. The emission was observed through a Corning 3-70 filter. Dots represent experimental points; the solid line is the calculated decay assuming the following parameters: α_1 = 0.48, τ_1 = 9.88 ns, α_2 = 0.52, and τ_2 = 22.3 ns with the reduced χ^2 = 1.044. The autocorrelation (top) and residuals (middle portion of the plot) are also shown. When a single-exponential was used to fit the data, the reduced value of χ^2 = 7.90.

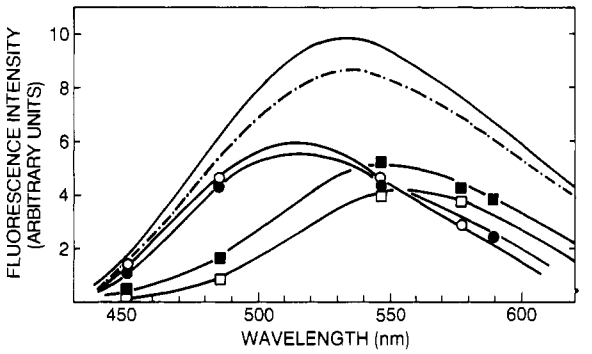

FIGURE 2: Decay-associated and steady-state spectra of dansylcadaverine conjugated with actin. Steady-state spectrum of G-actin (–·–) and F-actin (—). Long-lifetime component for G-actin (○); short-lifetime component for G-actin (□); long-lifetime component for F-actin (●); short-lifetime component for F-actin (■).

Table II: Fluorescence Decay Parameters for Dansylcadaverine F-Actin and Its Complexes with S1[a]

	actin ligand	α_1	τ_1 (ns)	α_2	τ_2 (ns)	$\langle\tau\rangle$ (ns)	$\langle E\rangle$ (%)
I[b]	none	0.44 ± 0.01	8.64 ± 0.01	0.56 ± 0.01	22.5 ± 0.1	19.3 ± 0.01	
	unlabeled S1	0.47 ± 0.01	8.76 ± 0.30	0.53 ± 0.01	21.7 ± 0.1	18.3 ± 0.04	
	TMR-LC_3–S1	0.54 ± 0.05	7.96 ± 0.05	0.49 ± 0.04	20.3 ± 0.1	16.7 ± 0.01	9.28
II[b]	none	0.59 ± 0.05	8.33 ± 0.14	0.41 ± 0.05	21.8 ± 0.12	17.1 ± 0.04	
	unlabeled S1	0.51 ± 0.03	8.05 ± 0.34	0.49 ± 0.03	18.3 ± 0.38	15.5 ± 0.06	
	TNP-S1	0.48 ± 0.17	6.88 ± 0.82	0.52 ± 0.16	17.8 ± 0.29	15.0 ± 0.09	3.73
III[b]	none	0.56 ± 0.03	8.55 ± 0.22	0.44 ± 0.03	22.1 ± 0.34	18.2 ± 0.90	
	IAA-S1	0.52 ± 0.04	8.59 ± 0.93	0.48 ± 0.04	21.0 ± 1.25	17.1 ± 0.92	
	(SH_1) TMR-S1	0.59 ± 0.06	7.00 ± 0.86	0.41 ± 0.06	19.3 ± 0.86	15.3 ± 0.03	10.9
IV	none[c,d] (n = 0.26)	0.45	6.27	0.55	22.9	19.9	
	none[c] (n = 0.96)	0.49	6.61	0.51	23.3	19.7	
V	none[e] (from DAS)		10.3		22.8		

[a] Samples were excited through a combination of Schott UG1 + UG11 filters with λ_{max} = 350 nm and $\Delta\lambda$ = 45 nm. [b] At 20 °C. Emission observed through a 486-nm interference filter. [c] Determined at 4 °C. [d] "Lightly" labeled sample. [e] From "global" analysis at five wavelengths at 4 °C.

The presence of the two components does not reflect an incomplete solvent relaxation around the dansyl chromophore. In such a case, the fluorescence maximum of the long-lifetime component is expected to be *red* shifted (McGregor & Weber, 1981), and we have confirmed that prediction for free dansylcadaverine in 99.8% glycerol at low temperature (data not shown). However, for the actin-bound label the long-lifetime component is *blue* shifted (Figure 2), which is the opposite of the observed shift for the free dye. Our observation is consistent with a model in which the dansyl chromophore undergoes heterogeneous interactions with the protein during the excited-state lifetime.

In 1,5-dansyl derivatives the emission can occur from either the ^1L_a or the ^1L_b state; which state is the emissive one depends on the environment (Li et al., 1975). In addition, dansylcadaverine possesses a long link between the chromophore and the protein backbone that facilitates penetration of different microenvironments surrounding Gln-41. The multiplicity of lifetimes can also be explained by assuming that the dye is immobile but interacts transiently with mobile aromatic residues or polar groups of the protein. An alternative approach is to interpret the data as indicative of a heterogeneous population of molecules.

While the available experimental data do not allow for distinguishing which of the above hypotheses is correct, all the proposed explanations share a common element: They require interactions of the dye with two or more different environments in the vicinity of the dye—environments that are generated by the protein structure.

To support further the conjecture that the protein structure is at least partially responsible for the two fluorescence components, we have measured the lifetimes of DNC–actin after having it denatured in 7 M Gdn-HCl. For the denatured sample we obtained $\alpha_1 = 0.99$, $\tau_1 = 5.69$ ns, $\alpha_2 = 0.01$, and $\tau_2 = 15.5$ ns. Since the 1% contribution of the 15.5-ns component is not significant, we have concluded that a well-defined protein structure is required for the existence of a nonnegligible fraction of the long-lifetime component.

Measurements of Transfer Efficiency. Elimination of Nondipolar Quenching Contributions. In order to eliminate quenching effects of S1 binding that are not due to the FRET phenomenon, we prepared IAA–S1 and examined its effect on the lifetime of the dansyl group when actin and S1 form the rigor complex. This experiment served as a control for energy-transfer measurements in which SH_1 has been labeled with ITMR. For experiments with TNP–S1 or TMR-LC_3, unmodified S1 was used. The quantum yield of the donor (dansylcadaverine) was determined as described under Materials and Methods; measurements done on two independently labeled samples yielded a value of 0.36 ± 0.01.

To ascertain that actin has been saturated with S1, a 2-fold molar excess of S1 over actin was used. As described under Materials and Methods, the efficiency of transfer has been determined from fluorescence lifetimes; Table II summarizes the results. The fitted parameters of the decay, α and τ, are highly correlated, and consequently, individual α's and τ's varied slightly from experiment to experiment. Much smaller variability was obtained for the mean lifetime of the decay $\langle\tau\rangle$, defined as

$$\langle\tau\rangle = \sum_i \alpha_i^2\tau_i / \sum_i \alpha_i\tau_i \qquad (5)$$

Therefore, we employed the mean lifetime to calculate the transfer efficiency. In each case reported, the FRET efficiency was low, indicating that either the donor–acceptor distance was long or the orientation of the dipoles participating in the transfer was highly unfavorable.

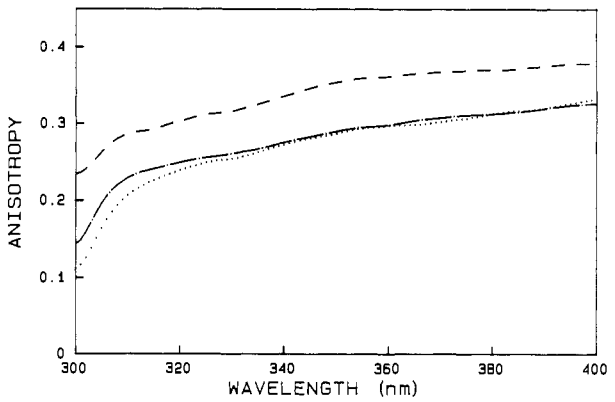

FIGURE 3: Fluorescence anisotropy excitation spectra for dansylcadaverine in 99.8% glycerol at −21 °C (−−), DNC–F-actin (20 μM) in 20 mM TES, 50 mM KCl, 1 mM $MgCl_2$, and 0.5 mM DTT, pH 7.5 at 20 °C (−·−), and DNC–F-actin (20 μM) + S1 (20 μM) at 20 °C (···).

Local Freedom of Probes. Estimation of Orientation Factor κ^2. The uncertainty in the calculated distances can be greatly reduced if one possesses information about the rotational freedom of the donor and the acceptor (Dale & Eisinger, 1974; Torgerson & Morales, 1984). Such analysis entails determination of the zero-time anisotropy for the chromophores participating in the transfer.

We have determined the limiting anisotropy for dansylcadaverine in 99.8% glycerol at −21 °C (Figure 3). If there were no local, depolarizing motion of the dye and if the protein segment to which the probe is attached were rigid, the polarization for DNC–actin should be equal to r_0 because one can neglect the motion of the polymerized actin (M_r >1 000 000). As seen from Figure 3, the anisotropy of DNC attached to actin has a markedly lower value, indicating that a rapid rotation of the chromophore takes place. According to Weber (1966) the angle of the rotation can be calculated from

$$r_x/r_0 = (3\cos^2\theta - 1)/2 \qquad (6)$$

where r_0 and r_x denote the anisotropy of viscosity immobilized and not immobilized, respectively. Upon substituting for r_0 = 0.351 at 348 nm and for r_x = 0.285, we obtain that the average angular displacement of the probe's dipole during fluorescence lifetime is 21°.

We have obtained fluorescence anisotropy spectra for TMR bound to Cys-136 (LC_3) and SH_1 in the acto–S1 complex as well as the limiting anisotropy for the TMR–β-mercaptoethanol adduct in 99.8% glycerol at −21 °C. There is practically no local motion of TMR attached to SH_1. In contrast, TMR on LC_3 rotates more freely. These findings are consistent with previous measurements of the local freedom of the probes attached to S1 but employing different dyes (Torgerson & Morales, 1984). Values of the limiting anisotropy of dansylcadaverine in 99.8% glycerol at −21 °C and the anisotropies of protein-bound probes were used to compute depolarization factors and limits for R_0 and the distances (Table III). The acceptor in the DNC–TNP pair is nonfluorescent, and the full Dale–Eisinger analysis cannot be performed. We assumed that we are dealing with the worst possible situation here; i.e., the acceptor is totally immobilized, $d_x = 1$.

Presence of Multiple Acceptors. When energy-transfer measurements are made on a multimeric protein such as F-actin, we have to consider a possibility of a transfer from one donor to more than one acceptor. This additional complication can be fully overcome by performing FRET measurements

Table III: FRET Parameters and Interprobe Distances from Gln-41 on Actin to Points on S1

parameter	S1 residue		
	SH_1	Cys-136 (LC_3)	RLR
J (nm^4 M^{-1} cm^{-1})	1.37×10^{15}	1.58×10^{15}	1.90×10^{13}
Q_D	0.36	0.36	0.36
d_x (donor)[a]	0.901	0.901	0.901
d_x (acceptor)[b]	0.999	0.883	1.0[c]
κ^2(min)	0.033	0.072	0.033
κ^2(max)	3.735	3.447	3.735
$R_0(2/3)$ (Å)	44.3	45.3	21.7
$\langle E \rangle$ (%)	10.9	9.28	3.73
r(min) (Å)	38.0	45.8	>22.5
$r_i(2/3)$ (Å)	63.1	66.3	>37.3
r(max) (Å)	83.7	87.2	>49.7

[a] Value at 348 nm in the presence of S1; in the absence of S1, d_x = 0.904; d_x is defined as $(r_x/r_0)^{1/2}$. [b] For LC_3 and SH_1 at 486 nm. [c] Nonfluorescent acceptor.

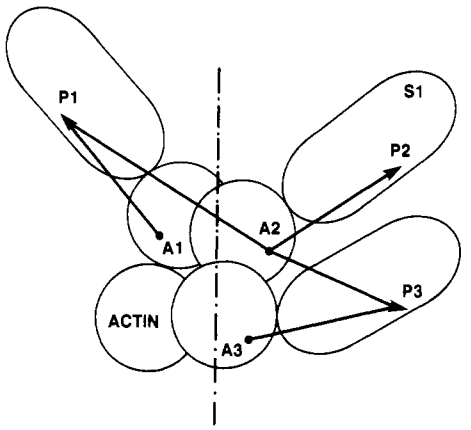

FIGURE 4: Schematic representation of three S1 molecules bound to the thin filament.

at various ratios of acceptor-labeled S1:unlabeled S1. In the present case the transfer is low even at saturating concentration of labeled S1, and it would drop below a measurable value if we decreased the concentration of labeled S1 severalfold. For this reason we have found this approach impractical.

A picture of the thin filament with three S1 molecules bound to it is shown in Figure 4. FRET may occur between donors A1, A2, and A3 on actin to the acceptors P1, P2, and P3 on S1. Donor A2 can transfer energy to P2, P3, and possibly P1. From the low efficiency of transfer it is evident that the distance is at least 37 Å (the shortest of the measured distances), so the distance A2–P1 must be longer; how much longer depends on the radial distance of the donor (the distance from the donor from the imaginary axis of the filament). We have determined the radial coordinate of Gln-41 in F-actin and found that its value corresponds to the location of Gln-41 on the surface of the filament (Kasprzak & Takashi, unpublished results). This fact has led us to the conclusion that the distance A2–P1 is substantially longer than A1–P1, and because A1–P1 is already long, the efficiency of FRET across the filament is negligible.

We now turn our attention to the transfer from donor A2 to acceptors P2 and P3 (Figure 4). If either A2–P2 $\gg$ A2–P3 or vice versa, FRET over the longer of the distances is eliminated because of the sixth root dependence in the Förster equation. The largest error is made when A2–P2 = A2–P3. In that case each donor is transferring energy to two acceptors, but we compute the distance assuming that only one acceptor is involved.

Cases with multiple acceptors have been dealt with before (Bay & Pearlstein, 1963; Gennis & Cantor, 1972), and a general equation for a multiple transfer has been derived:

$$E = \sum_i (R_0/r_i)^6 / [1 + \sum_i (R_0/r_i)^6] \quad (7)$$

where N is the number of acceptors. For two equidistant acceptors, this equation reduces to

$$r_i = R_0(2^{1/6})[(1 - E)/E]^{1/6} \quad (8)$$

If eq 4 is used to compute distances instead of eq 7, the distance that is obtained is $2^{1/6} = 1.12$ times shorter; in the worst case, therefore, the relative error of the distance due to the presence of two acceptors is 12%. Although error of that magnitude is not negligible, the multiacceptor transfer does not change any of the conclusions we have reached in this paper.

Conclusions

In this paper we report three new distances between points on actin and points on S1 in the rigor complex. The chemical point on actin was in each case Gln-41, a residue located in the "small" domain of actin. Cross-linking experiments (Mornet et al., 1981) have suggested that this domain has an S1 binding site on its N-terminus (Sutoh, 1982). Gln-41, however, seems to be quite remote from that site, and it is presumably located near the actin–actin interface but not at the interface. This suggestion is based on the observation that fluorescence of the DNC–actin is strongly dependent on the polymerization state of the protein and is consistent with the finding that modification of the neighboring His-40 impairs polymerization of G-actin (Hegyi et al., 1974). Since actin can be transglutaminase-labeled in both forms (G and F), a direct involvement of the actin–actin interface residues seems unlikely.

Our data are not consistent with the results of the proton NMR study of the interaction between S1 and peptide CB13 of actin, containing residues 1–44 (Moir et al., 1987). The conclusion reached in that paper was that the C-terminal region of the CB13 peptide is less than 12 Å away from the SH_1 group and is directly perturbed by S1 residues. Although we cannot explain the disagreement in the distance estimation, we note that a small quenching effect of S1 on the fluorescence of DNC–actin indicates that the binding of S1 is indeed sensed by the dye attached to Gln-41. Nevertheless, this effect appears to be indirect; i.e., S1 does not enter into a direct contact with the aromatic portion of the probe since the affinity of S1 for actin is unaffected by the modification (Takashi, 1987) and the rotational mobility of dansyl is unchanged by the S1 binding (Figure 3).

The fluorescence of dansylcadaverine conjugated to either F-actin or G-actin has two lifetime components. The presence of two exponential terms in the fluorescence decay of 1,5-IAEDANS-labeled actin (at Cys-374) has been observed before (Torgerson & Morales, 1984). Betteridge and Lehrer (1983) reported two decay components for dansylcystine-labeled cardiac tropomyosin. They interpreted the existence of the double-exponential decays as a manifestation of two protein conformations. However, in any of the above cases, including ours, it has not been established whether the occurrence of two lifetime components is a result of the interaction of the label with two different regions of the protein or there exist two different protein conformations that the probe detects. Further experiments are required to clarify this point.

The overall focus of this research is to determine the relative location of points in the acto–S1 complex. One of the distances reported here, viz., DNC–actin to RLR, has been based on a 3.73% transfer efficiency. We feel that such a low FRET cannot be reliably measured and it is likely that the value of

37 Å (Table III) represents a lower limit for this D–A distance.

The length and the flexibility of the link between the aromatic ring of the chromophore and its attachment site to protein raise the possibility that in our system FRET measures an average donor–acceptor distance without any physical meaning because the distribution of these distances is not known. However, a wide distribution of distances should manifest itself as a markedly nonexponential decay, especially at short times after excitation. Such behavior was observed when an ensemble of donors and acceptors was placed in a membrane or vesicle (Fung & Stryer, 1978), but we have never seen it when distances between actin and S1 have been measured. Hence, we conclude that in our case the distribution of distances is narrow and the use of a single value for the D–A distance is meaningful.

In spite of the above uncertainties concerning the measured distances, the qualitative conclusions from this paper are quite clear: In the acto–S1 rigor complex the distance from Gln-41 on actin to RLR is longer than 37 Å, and SH_1 of S1 and Cys-136 of LC_3 are about 65 Å away from Gln-41 on actin.

The results described in this paper in conjunction with other distances already reported can be utilized for proximity mapping in the contractile protein system. The most promising applications are the following: (1) orientation of S1 with respect to the thin filament when the structure of actin becomes available; (2) examination of a possible interprotein motion when a weakly dissociating nucleotide such as Mg·ADP is added; (3) a reconstruction of the three-dimensional structure of S1 with data from high-resolution NMR measurements. These are constraints provided by FRET and the distance–geometry algorithm (Wüthrich et al., 1982; Brünger et al., 1987).

ACKNOWLEDGMENTS

We thank Professor Manuel F. Morales for his advice and helpful discussions concerning various aspects of this work. We gratefully acknowledge critical comments of Dr. Patrick Chaussepied and Dr. Julian Borejdo.

REFERENCES

Badea, M. G., & Brand, L. (1979) *Methods Enzymol. 61*, 378–425.

Bay, Z., & Pearlstein, R. M. (1963) *Proc. Natl. Acad. Sci. U.S.A. 50*, 1071–1078.

Betteridge, D. R., & Lehrer, S. S. (1983) *J. Mol. Biol. 167*, 481–496.

Botts, J., Takashi, R., Torgerson, P., Hozumi, T., Muhlrad, A., Mornet, D., & Morales, M. F. (1984) *Proc. Natl. Acad. Sci. U.S.A. 81*, 2060–2064.

Brünger, A. T., Campbell, R. L., Clore, G. M., Gronenborn, A. M., Karplus, M., Petsko, G. A., & Teeter, M. M. (1987) *Science (Washington, D.C.) 235*, 1049–1053.

Cheung, H. C., Gonsoulin, F., & Garland, F. (1983) *J. Biol. Chem. 258*, 5775–5786.

Connellan, J. M., Chung, S. I., Whetzel, K., Bradley, L. M., & Folk, J. E. (1971) *J. Biol. Chem. 246*, 1093–1098.

Dalbey, R. E., Weiel, J., & Yount, R. G. (1983) *Biochemistry 22*, 4696–4706.

Dale, R. E., & Eisinger, J. (1974) *Biopolymers 13*, 1573–1605.

Dos Remedios, C. G., & Cooke, R. (1984) *Biochim. Biophys. Acta 788*, 193–205.

Elzinga, M., & Collins, J. H. (1977) *Proc. Natl. Acad. Sci. U.S.A. 74*, 4281–4284.

Elzinga, M., Collins, J. H., Kuehl, W. M., & Adelstein, R. S. (1973) *Proc. Natl. Acad. Sci. U.S.A. 70*, 2687–2691.

Frank, G., & Weeds, A. G. (1974) *Eur. J. Biochem. 44*, 317–334.

Fung, B. K.-K., & Stryer, L. (1978) *Biochemistry 17*, 5241–5248.

Gallagher, M., & Elzinga, M. (1980) *Fed. Proc., Fed. Am. Soc. Exp. Biol. 39*, 2168.

Gennis, R. B., & Cantor, C. R. (1972) *Biochemistry 11*, 2509–2517.

Grinvald, A., & Steinberg, I. Z. (1974) *Anal. Biochem. 59*, 583–598.

Holt, J. C., & Lowey, S. (1975) *Biochemistry 14*, 4600–4609.

Houk, T. W., & Ue, K. (1974) *Anal. Biochem. 62*, 66–74.

Li, Y.-H., Chan, L.-M., Tyer, L., Moody, R. T., Himmel, C. M., & Hercules, D. M. (1975) *J. Am. Chem. Soc. 97*, 3118–3126.

Lorand, L., Rule, N. G., Ong, H. H., Furlanetto, R., Jacobsen, A., Downey, J., Oner, N., & Bruner-Lorand, J. (1968) *Biochemistry 7*, 1214–1223.

Lowry, O. H., Rosenbrough, N. J., Farr, A. L., & Randall, R. J. (1951) *J. Biol. Chem. 193*, 265–275.

Margossian, S. S., Stafford, W. F., & Lowey, S. (1981) *Biochemistry 20*, 2151–2155.

Marsh, D. J., & Lowey, S. (1980) *Biochemistry 19*, 774–784.

McGregor, R. B., Jr., & Weber, G. (1981) *Ann. N.Y. Acad. Sci. 366*, 140–154.

Mendelson, R., Putnam, S., & Morales, M. (1975) *J. Supramol. Struct. 3*, 162–168.

Miki, M., & Mihashi, K. (1978) *Biochim. Biophys. Acta 533*, 163–172.

Miki, M., & Wahl, P. (1984) *Biochim. Biophys. Acta 786*, 188–196.

Moir, A. J. G., Levine, B. A., Goodearl, A. J., & Trayer, I. P. (1987) *J. Muscle Res. Cell Motil. 8*, 68.

Moore, P. B., Huxley, H. E., & DeRosier, D. J. (1970) *J. Mol. Biol. 188*, 595–612.

Mornet, D., Bertrand, R., Pantel, P., Audemard, E., & Kassab, T. (1981) *Nature (London) 292*, 301–306.

Moss, D. J., & Trentham, D. R. (1983) *Biochemistry 22*, 5261–5270.

Muhlrad, A., & Takashi, R. (1981) *Biochemistry 20*, 6749–6754.

Okuyama, T., & Satake, K. (1960) *J. Biochem. (Tokyo) 47*, 454–466.

Ross, J. B. A., Schmidt, C. J., & Brand, L. (1981) *Biochemistry 20*, 4369–4377.

Scott, T. G., Spencer, R. D., Leonard, N. J., & Weber, G. (1970) *J. Am. Chem. Soc. 92*, 687–695.

Spencer, R. D., & Weber, G. (1970) *J. Chem. Phys. 52*, 1654–1663.

Spudich, J. A., & Watt, S. (1971) *J. Biol. Chem. 246*, 4866–4871.

Sutoh, K. (1982) *Biochemistry 21*, 3654–3661.

Sutoh, K., Yamamoto, K., & Wakabayashi, T. (1984) *J. Mol. Biol. 178*, 323–339.

Sutoh, K., Yamamoto, K., & Wakabayashi, T. (1986) *Proc. Natl. Acad. Sci. U.S.A. 83*, 212–216.

Takashi, R. (1979) *Biochemistry 18*, 5164–5169.

Takashi, R. (1987) *Biochemistry* (in press).

Takashi, R., & Kasprzak, A. A. (1985) *Biophys. J. 47*, 26a.

Takashi, R., Duke, J., Ue, K., & Morales, M. F. (1976) *Arch. Biochem. Biophys. 175*, 279–283.

Takashi, R., Muhlrad, A., & Botts, J. (1982) *Biochemistry 21*, 5661–5668.

Takashi, R., Torgerson, P., & Duke, J. (1984) *Biophys. J. 45*, 223a.

Tao, T., & Lamkin, M. (1981) *Biochemistry 20*, 5051–5055.

Taylor, K. A., & Amos, L. A. (1981) J. Mol. Biol. 147, 297–324.
Tong, S. W., & Elzinga, M. (1983) J. Biol. Chem. 258, 13100–13110.
Torgerson, P. M. (1984) Biochemistry 23, 3002–3007.
Torgerson, P. M., & Morales, M. F. (1984) Proc. Natl. Acad. Sci. U.S.A. 81, 3723–3727.
Toyoshima, C., & Wakabayashi, T. (1985) J. Biochem. (Tokyo) 97, 219–243.
Trayer, H. R., & Trayer, I. P. (1983) Eur. J. Biochem. 135, 47–59.
Wagner, P. D., & Weeds, A. G. (1977) J. Mol. Biol. 109, 455–473.
Weber, G. (1966) in Fluorescence and Phosphorescence Analysis (Hercules, D. M., Ed.) pp 217–240, Interscience, New York.
Weeds, A. G., & Taylor, R. S. (1975) Nature (London) 257, 54–56.
Winkelmann, D. A., & Lowey, S. (1986) J. Mol. Biol. 188, 595–612.
Wüthrich, K., Wider, G., Wagner, G., & Braun, W. (1982) J. Mol. Biol. 155, 311–319.

Further Characterization of the Interaction of Histidine-Rich Glycoprotein with Heparin: Evidence for the Binding of Two Molecules of Histidine-Rich Glycoprotein by High Molecular Weight Heparin and for the Involvement of Histidine Residues in Heparin Binding†

Mary Kappel Burch,‡,§ Michael N. Blackburn,‖ and William T. Morgan*,‡

Department of Biochemistry and Molecular Biology, Louisiana State University Medical Center, New Orleans, Louisiana 70112, and Department of Biochemistry and Molecular Biology, Louisiana State University Medical Center, Shreveport, Louisiana 71130

Received November 26, 1986; Revised Manuscript Received July 14, 1987

ABSTRACT: Rabbit histidine-rich glycoprotein (HRG, 94 kDa) binds heparin with high affinity (apparent K_d 60–110 nM). Eosin Y (1 equiv) bound to HRG was used as a reporter group to monitor associations of HRG with heparins of molecular mass 10, 17.5, and 30 kDa. The stoichiometries of the heparin–HRG complexes were determined by fluorescence and absorbance measurements as well as by analytical ultracentrifugation. Two types of complex form: complexes of 1 heparin:1 HRG and of 1 heparin:2 HRG. The 1:2 complex formation requires a minimum heparin chain length since 17.5-kDa but not 10-kDa heparin binds two HRG molecules. The formation of the 1:2 complexes of the larger heparin fractions is enhanced by divalent copper or zinc (1–10 equiv) bound to HRG. However, metal is not required for complex formation since all sizes of heparin examined interact tightly with HRG in the presence of ethylenediaminetetraacetic acid. Between 0.1 and 0.3 M ionic strength, both 1:1 and 1:2 complexes of heparin with HRG are progressively destabilized. No heparin–HRG complex is found at ionic strengths of 0.5 M. Between pH 8.5 and pH 6.5 both 1:2 and 1:1 complexes are found with 17.5-kDa heparin, but at pH 5.5 only 1:1 complexes are formed. The heparin–HRG interaction is progressively decreased by modification of the histidine residues of HRG, whereas modification of 22 of the 33 lysine residues of HRG has little effect. Supporting the role of histidine in heparin binding, a histidine–proline–glycine-rich peptide (molecular mass 28 kDa) derived from HRG and intact HRG binds to heparin–Sepharose at pH 6.8, but only HRG binds to the affinity medium at pH 7.4.

Histidine-rich glycoprotein (HRG) is a serum protein known to interact with heparin (Koide et al., 1982), plasminogen (Lijnen et al., 1980), thrombospondin (Leung et al., 1984), fibrinogen and fibrin (Leung, 1986), metal ions (Cu^{2+}, Zn^{2+}, Ni^{2+}, Co^{2+}) (Guthans & Morgan, 1982), and iron porphyrins (Morgan, 1978, 1981). Despite these known associations in vitro, the physiological function of HRG remains unclear. The interaction of human HRG with the anticoagulant heparin (a single-stranded negatively charged polysaccharide) has been the subject of several studies. The heparin binding activity of HRG has been examined indirectly by monitoring the formation of platelet aggregates (Kindness et al., 1984) and the inhibition of proteases by antithrombin III (Lijnen et al., 1983; Lane et al., 1986) and heparin cofactor II (Tollefsen & Pestka, 1985). HRG was found to bind heparin with similar affinity to antithrombin III and platelet factor 4 (Tollefsen & Pestka, 1985) and to bind dermatan sulfate only weakly. In addition, HRG binds heparin of molecular weight larger than 5400 better than smaller forms and has no preference for high-affinity heparin (Lane et al., 1986). In view of the known metal-binding ability of HRG,

† This work was supported in part by the National Institutes of Health under Fellowship GM-09797 to M.K.B. and Grants HL-24846 to M.N.B. and HL-37570 to W.T.M.

* Address correspondence to this author at the Department of Biochemistry and Molecular Biology, Louisiana State University Medical Center, New Orleans, LA 70112.
‡ Louisiana State University Medical Center, New Orleans.
§ Present address: Rohm and Haas, Inc., Spring House, PA 19477.
‖ Louisiana State University Medical Center, Shreveport.

0006-2960/87/0426-7477$01.50/0